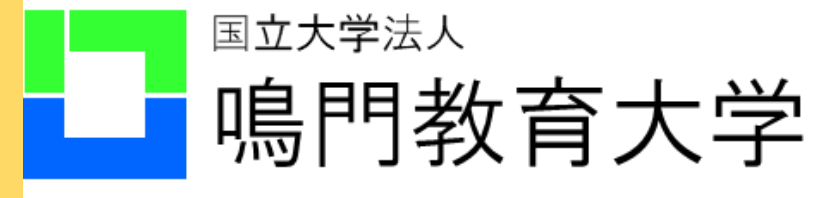


# Numerical analysis of isotope effect in NIFS negative ion source

Ryo Kato<sup>1</sup>, Kazuo Hoshino<sup>1</sup>, Haruhisa Nakano<sup>2</sup>, Takanori Shibata<sup>3</sup>, Kenji Miyamoto<sup>4</sup>, Kengo Iwanaka<sup>1</sup>, Katsuya Hayashi<sup>1</sup>, Akiyoshi Hatayama<sup>1</sup>



<sup>1</sup>Faculty of Science and Technology, Keio University, Yokohama, Japan  
<sup>2</sup>National Institute for Fusion Science, National Institutes of Natural Science, Toki, Japan  
<sup>3</sup>Accelerator Laboratory, KEK, Tsukuba, Japan  
<sup>4</sup>Graduate School of Education, Naruto University of Education, Naruto, Japan



## Summary

- In hydrogen (H) and deuterium (D) experiments in NIFS-RNIS, **increase in co-extracted electron current is observed.**
- For **analysis of isotope effects** in the ion source through electron transport simulation, 3D kinetic particle tracking model **KEIO-MARC code was modified for application to NIFS-RNIS.**
- KEIO-MARC code **reproduced basic characteristics**, such as electron flow by magnetic drift, filter effect, etc. and calculated EEDF, electron density, electron temperature, and reaction frequency.
- The **isotope effects via following process** was analyzed and we concluded that **other isotope effects are the reason of difference in electron density.**
  - Sheath potential drop** at the chamber wall **did not produce large difference in electron density.**
  - Coulomb collision** **did not produce large difference in electron density.**
  - Some reactions** between ground state atoms and molecules **did not produce large difference in electron density.**

## 1. Introduction

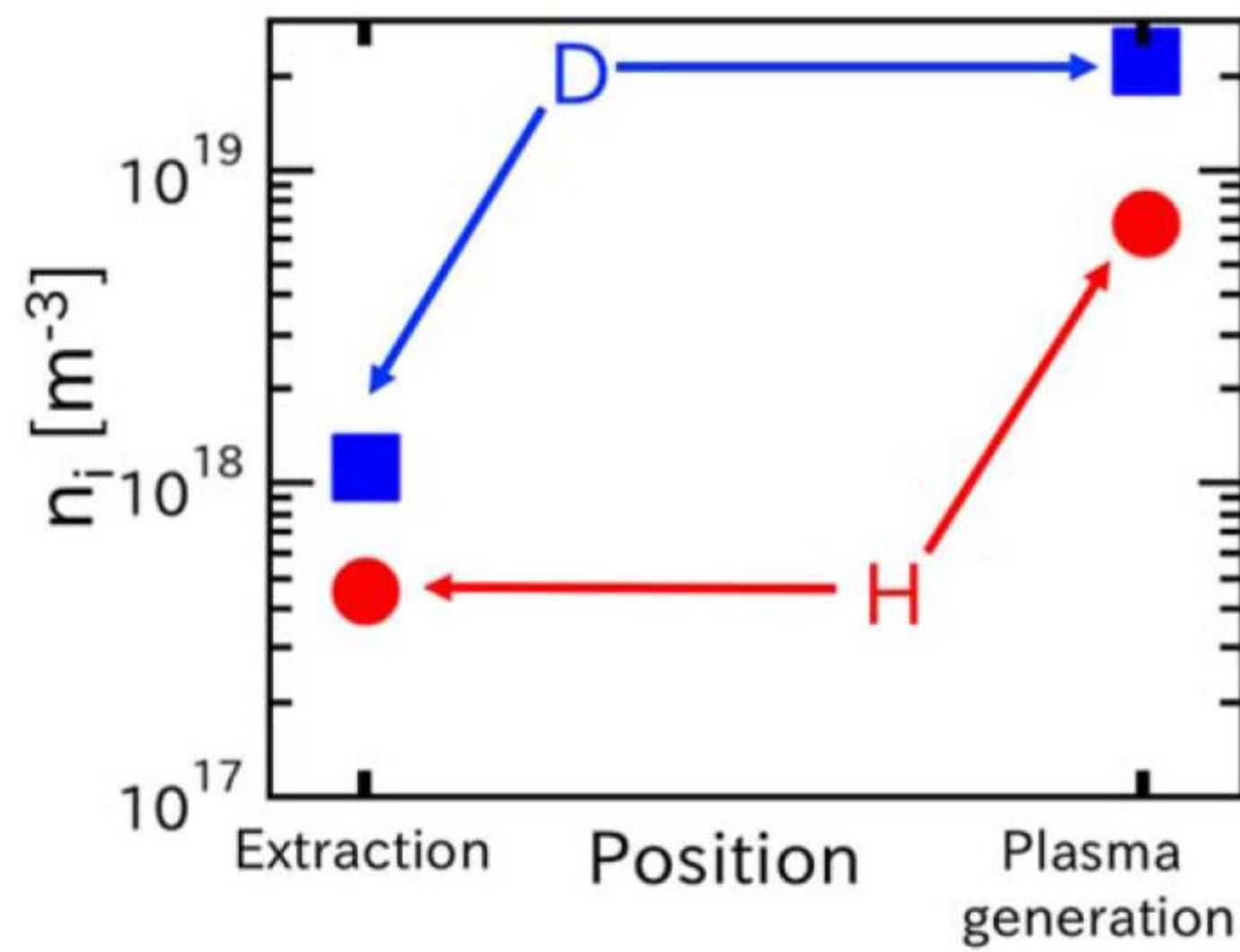


Fig. 1 Result of NIFS-RNIS experiment [1]

- In hydrogen (H) and deuterium (D) experiments in NIFS-RNIS (negative ion source for experiment), the **electron density** in both extraction and plasma generation region is **higher in the D plasma than that of H plasma by a factor of around 3.**[1]
- This will lead to NBI (Neutral Beam Injection) beam power limitation due to larger heat load by co-extracted electron current and needs to be improved.

### Purpose

Investigation of high electron density in D plasma through electron transport simulation.

### In this paper

Analysis of the isotope effect on 1. sheath potential drop, 2. coulomb collision, and 3. some reactions.

## 2. Simulation Model

### KEIO-MARC code[2,3]

**Kinetic modeling of Electrons in the IO source plasmas by the Multi-cusp ARC-discharge code**

KEIO-MARC code is a 3D kinetic particle tracking model which simulates electron transport through equation of motion.

$$m_e \frac{dv_e}{dt} = -ev_e \times B + (\text{collision force})$$

※  $E = 0$  by assuming quasi-neutral plasma in the chamber.

Considers...

- 3D shape of the target device.
- 3D magnetic configuration.
- Reflection at the chamber wall by **sheath potential**.
- Coulomb collisions.**
  - 2 types of collisions: electron – electron collision and electron -  $H^+$  collision.
  - $H^+$  density will be same as electron density by assuming quasi-neutral plasma because  $H^+$  is treated as background plasma in this model.
- Both elastic and inelastic collisions.**
  - $H_2, H^0, H^+, H_2^+, H_3^+$  are treated as background plasma. Density and temperature are given as a set parameter and spatial distribution is set to be uniform in the chamber.
  - When electron production reactions occurs, it produces 1 test particle (electron) at the reaction position and produced particle will be tracked as well.
  - When electron reduction reactions occurs, that test particle is lost at the reaction position.

Electron Energy Distribution Function (EEDF) is calculated for each spatial cell

### NIFS-RNIS

Target device is **R&D negative ion source NIFS-RNIS.**

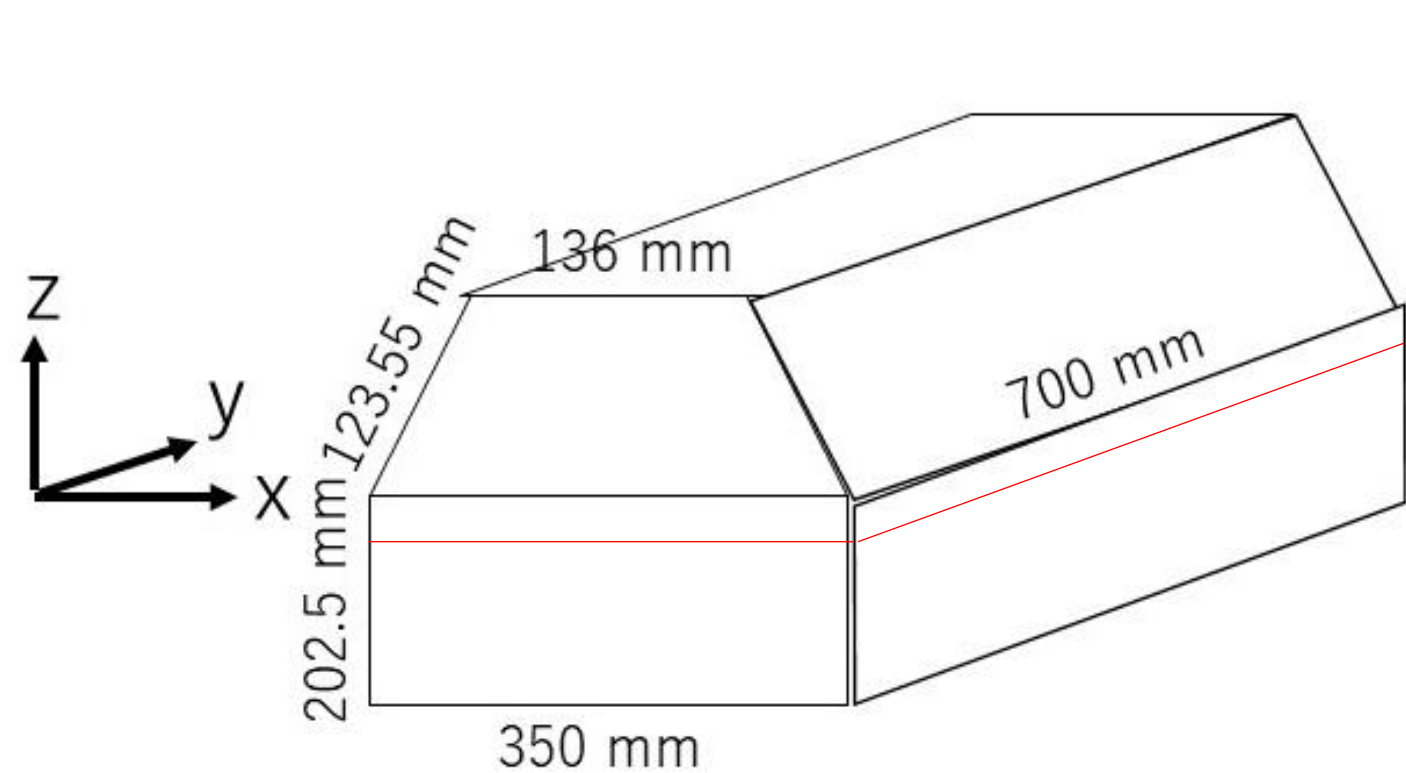


Fig. 2 Arc chamber dimension of NIFS-RNIS

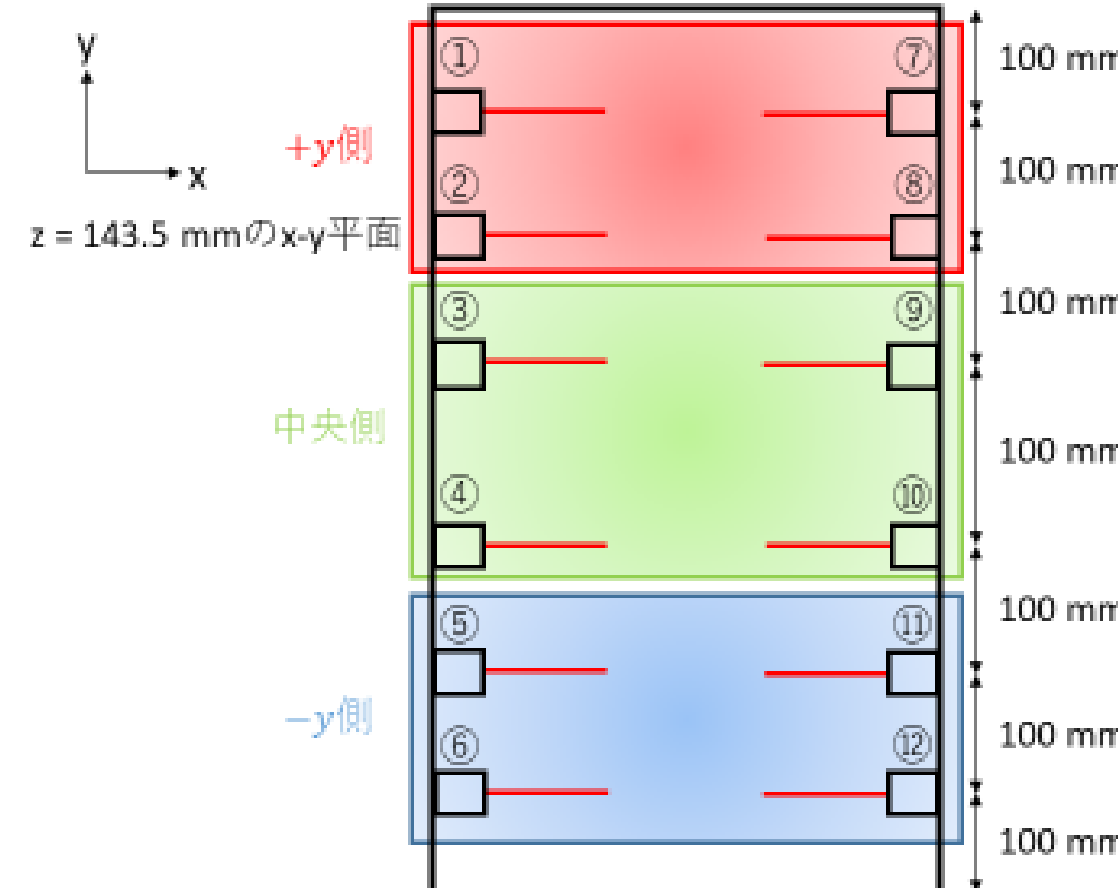


Fig. 3 Filament position

- +Z axis direction : Opposite of beam extraction direction
- +X axis direction : Parallel to filter magnetic field

### Calculation Conditions

- Time step width :  $10^{-10}$  [s]
- Time step number : 900,000
- Extraction holes :  $z = 0$
- Weight of test particle :  $3.13 \times 10^{13}$

Table 1 Arc-discharge conditions

Arc Power	8300 W
Arc Voltage	82 V
H <sub>2</sub> Gas Pressure	0.3 Pa

Table 2 Background plasma

Particles	Density [m <sup>-3</sup> ]	Temperature [K]
H <sub>2</sub>	$1.68 \times 10^{18}$	774
H <sup>0</sup>	$1.68 \times 10^{17}$	774
H <sup>+</sup>	$4 \times 10^{17}$	457
H <sub>2</sub> <sup>+</sup>	$1 \times 10^{17}$	457
H <sub>3</sub> <sup>+</sup>	$5 \times 10^{17}$	457

## 3. Results and Discussion

### Application to NIFS-RNIS

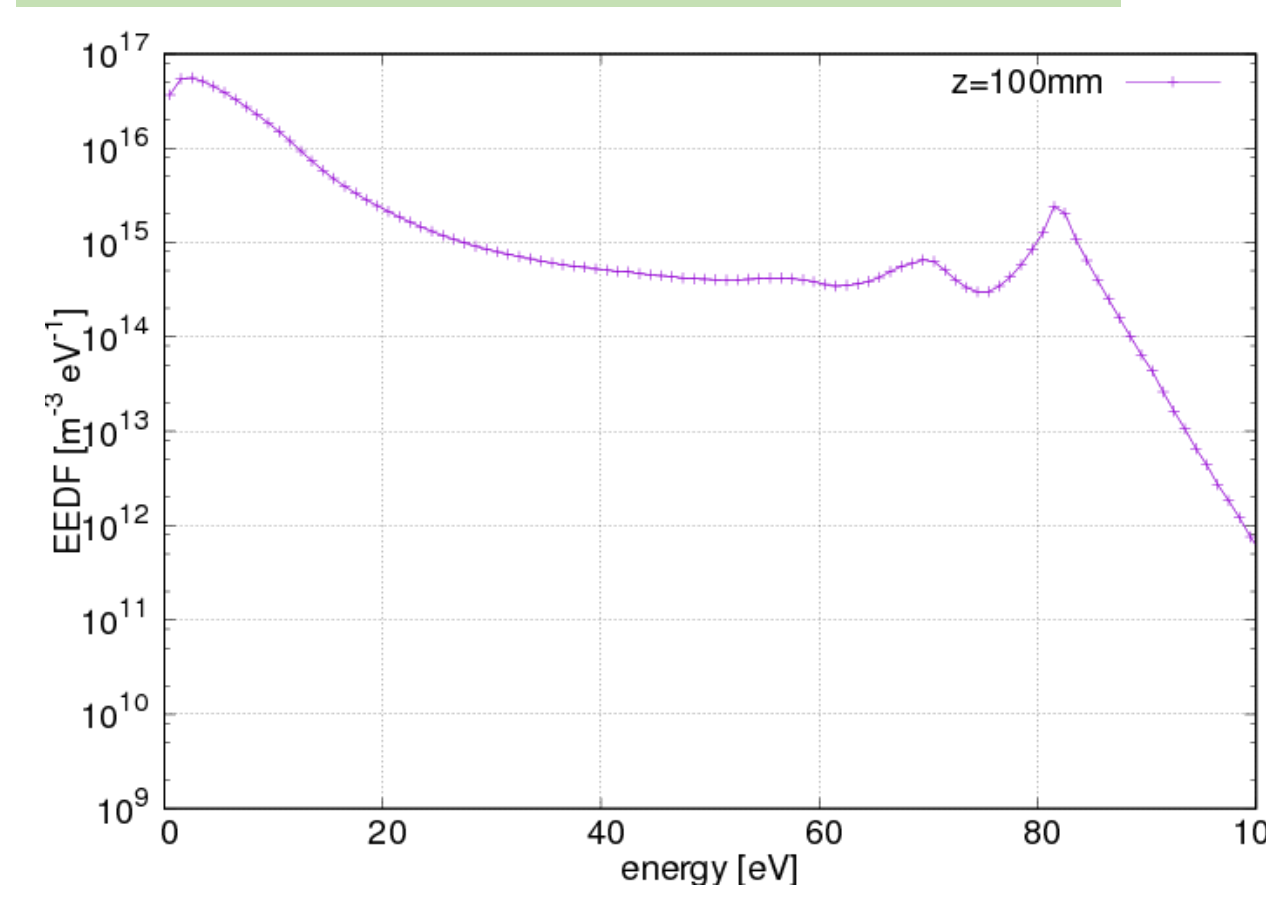


Fig. 4 EEDF

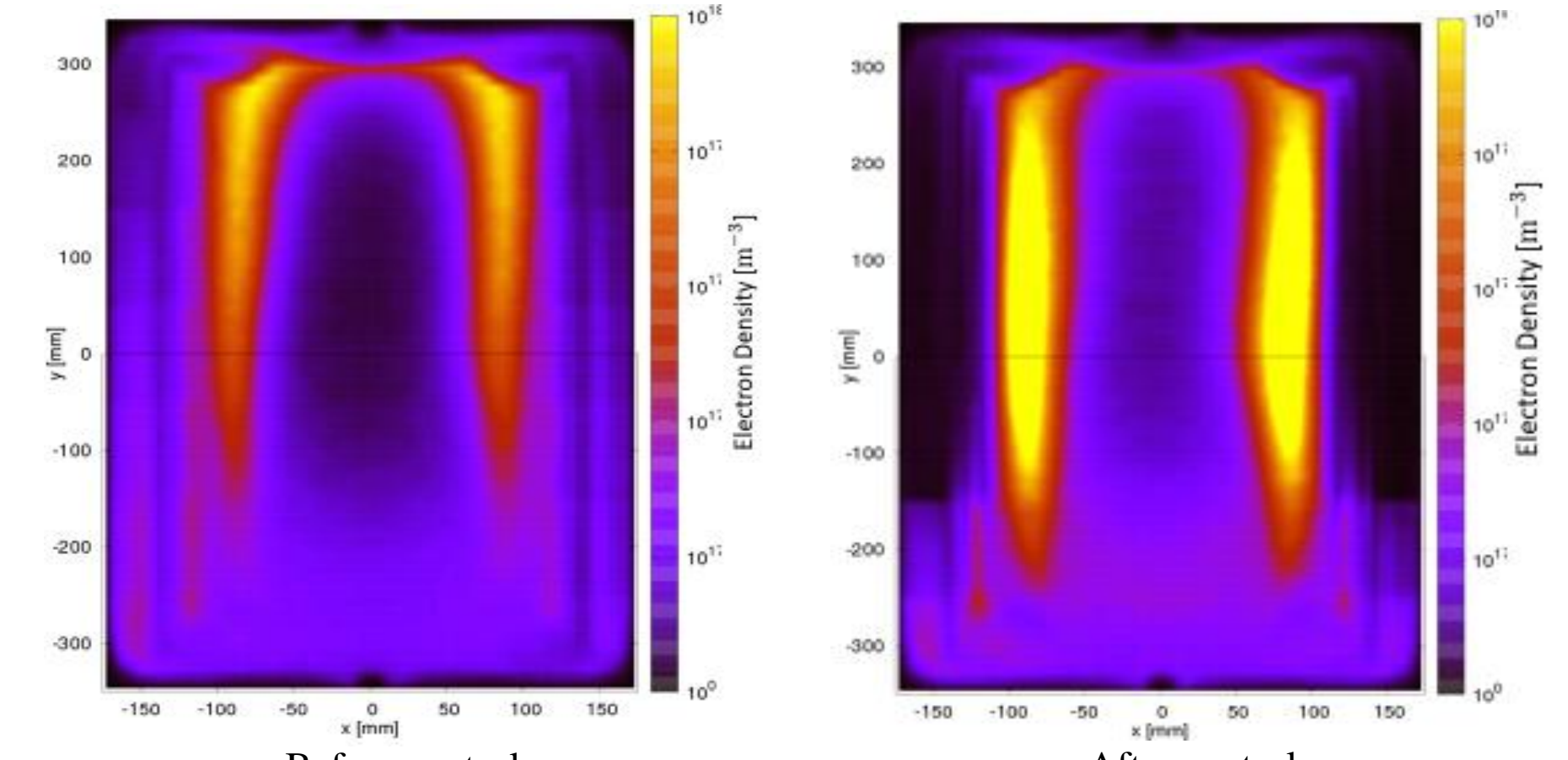


Fig. 5  $n_e$  distributions in xy plane at  $z = 142$  mm (near filament)

Table 3 Production Reactions

Nondissociative Ionization	$e + H_2(X^1\Sigma_g^+) \rightarrow H_2^+ + 2e$
H(1s) Ionization	$e + H(1s) \rightarrow H^+ + 2e$
H <sub>2</sub> <sup>+</sup> Dissociation 1	$e + H_2^+ \rightarrow H^+ + H^+ + 2e$
Dissociative Ionization	$e + H_2(X^1\Sigma_g^+; v=0) \rightarrow H^+ + H(1s) + 2e$

Table 4 Reduction Reactions

Dissociative Attachment	$e + H_2(v) \rightarrow H + H^-$
H <sub>2</sub> <sup>+</sup> Dissociation 3	$e + H_2^+ \rightarrow H(1s) + H^+$
H <sub>2</sub> <sup>+</sup> Dissociative Recombination	$e + H_2^+ \rightarrow 3H(1s)$

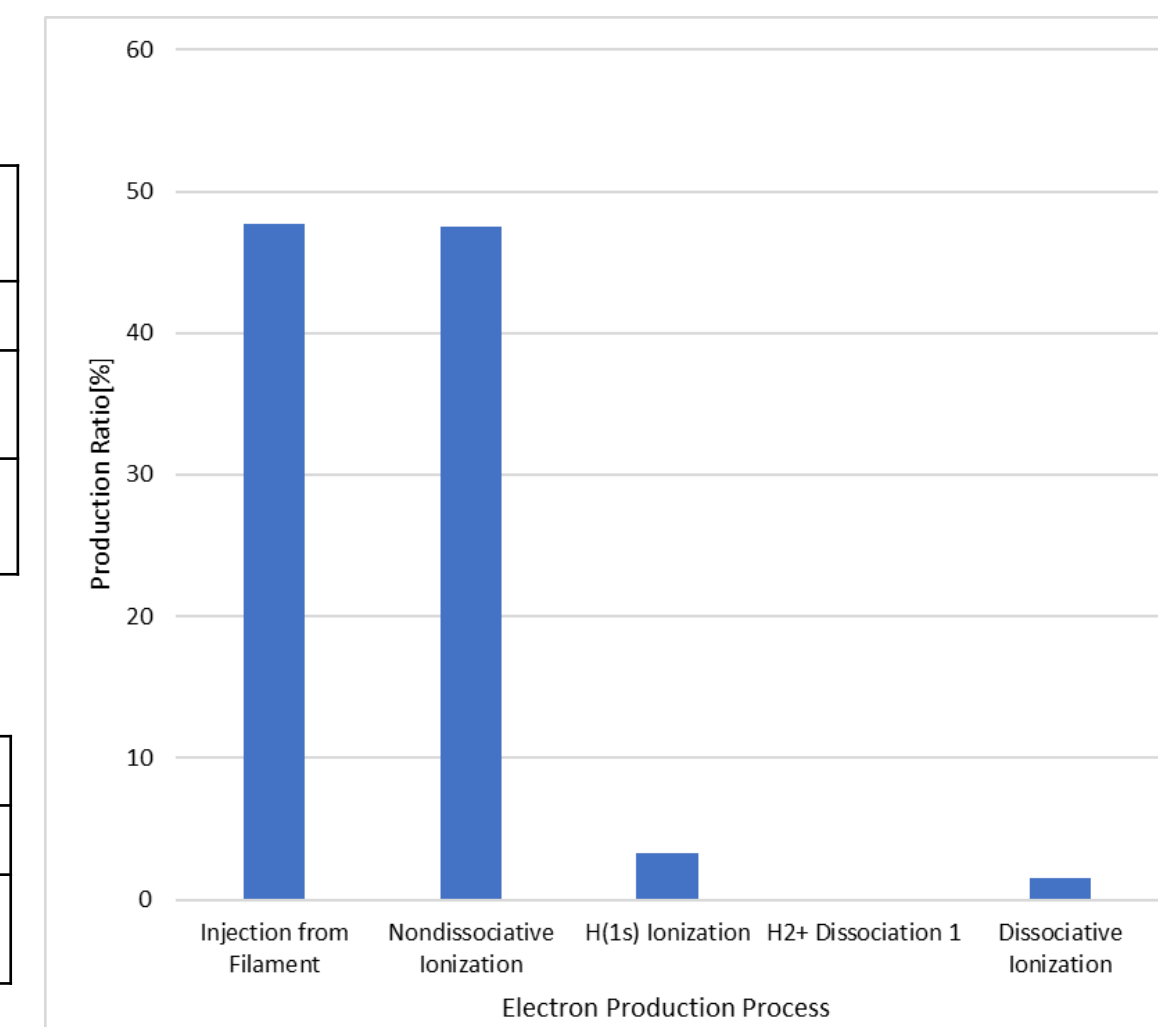


Fig. 6 Ratio of electron production process

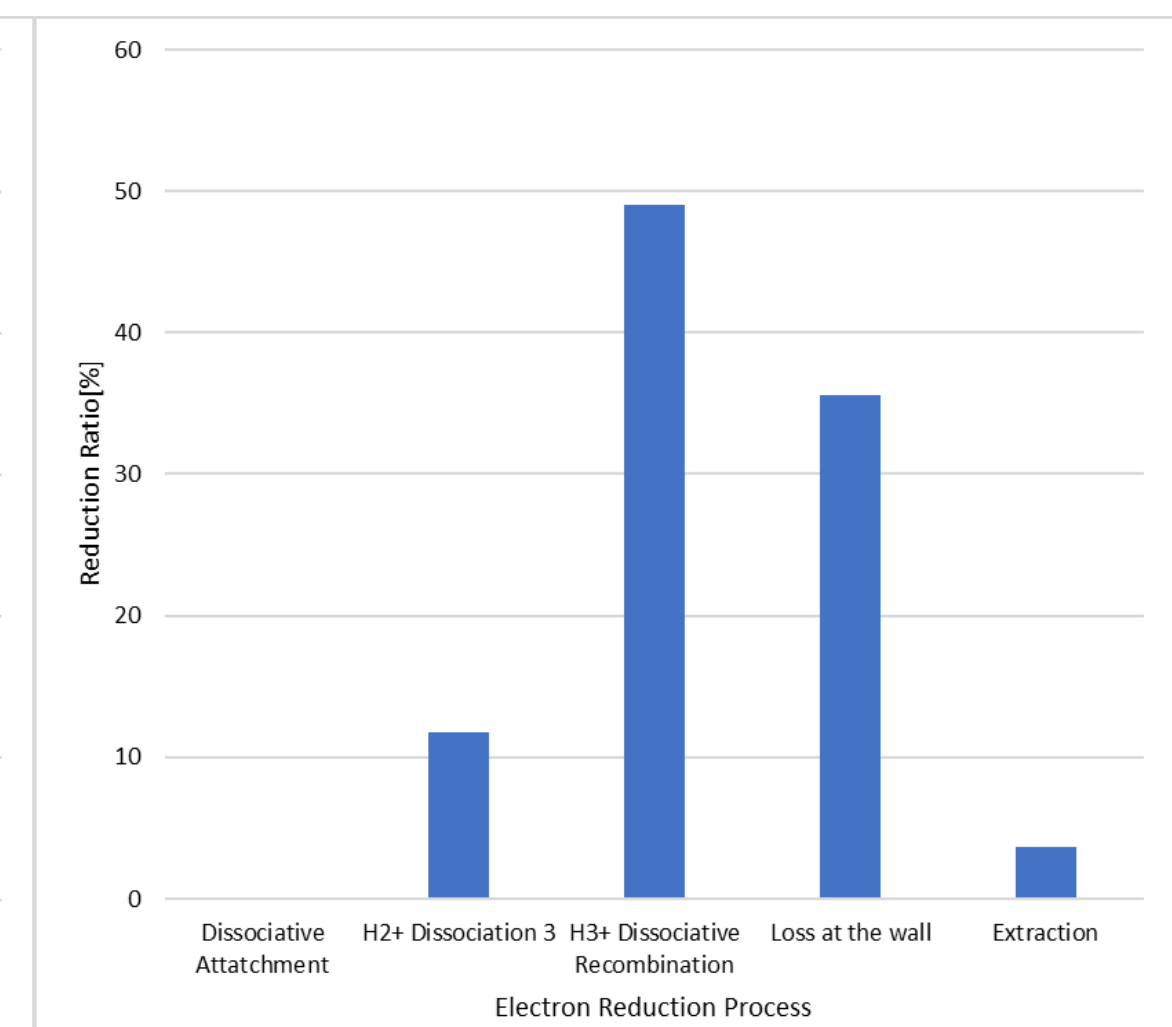


Fig. 7 Ratio of electron reduction process

- In EEDF, peak at 83 V (arc voltage) is observed.
- Filament injection control done in NIFS-RNIS to counter grad B drift is reproduced.
- Injection from filament** and **nondissociative ionization** are the 2 dominant electron production process.
- H<sub>2</sub><sup>+</sup> dissociative recombination** is the dominant electron reduction process, followed by loss at the wall.

### 1. Isotope effect on sheath potential drop

- Depth of sheath potential :

$$\Phi_{sh} = \frac{k_B T_e}{2e} \ln \left( \frac{m_i}{2\pi m_e} \right)$$

- Isotope effect on sheath potential drop is **not the reason of electron density increase.**

Table 5 Isotope effect on sheath potential drop

Electron Density Ratio	Electron Temperature Ratio
104.41%	99.57%

### 2. Isotope effect on coulomb collision

- Mass of collision partner :  $m_{H^+} \rightarrow m_{D^+}$

- Isotope effect on coulomb collision is **not the reason of electron density increase.**

Table 6 Isotope effect on coulomb collision

Electron Density Ratio	Electron Temperature Ratio
100.05%	100.24%

### 3. Isotope effect on reactions

- Cross section
- Mass of collision partner

Table 7 Isotope effect on reactions

Reaction	Electron Density Ratio	Electron Temperature Ratio	
DI	$e + H_2(X^1\Sigma_g^+; v=0) \rightarrow e + H^+ + H(1s)$	99.81%	100.09%
Nondiss IOZ	$e + H_2(X^1\Sigma_g^+) \rightarrow e + H_2^+ + e$	99.40%	100.94%
DA	$e + H_2(v) \rightarrow H + H^-$	99.96%	100.02%
eV①	$e + H_2(X^1\Sigma_g^+; v=0) \rightarrow e + H_2(X^1\Sigma_g^+; v=1)$	97.38%	97.66%
eV②	$e + H_2(X^1\Sigma_g^+; v=0) \rightarrow e + H_2(X^1\Sigma_g^+; v=2)$	100.25%	99.01%
e Excitation	$e + H_2(X^1\Sigma_g^+) \rightarrow e + H_2^*(B^1\Sigma_u^+)$	105.07%	100.51%

- Isotope effect on these 7 reactions are **not the reason of electron density increase.**

## 4. Development Plans and Discussion

Following factors need to be considered...

- Difference of energy loss through each reactions.
- Difference of threshold energy.
- Isotope effect of other reactions.
- Reactions of vibrationally excited molecules.
- Difference of vibrationally excited levels of molecules.
- Ambipolar diffusion

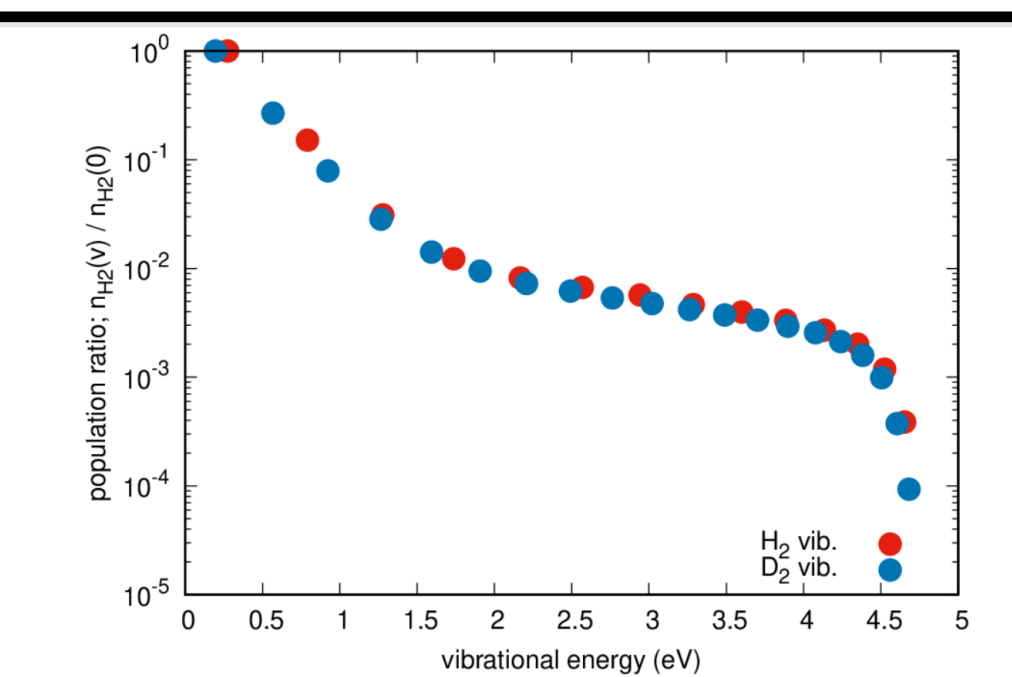


Fig. 8 Difference of ionization channel [4]

Calculation of the zero-dimensional model suggests that **difference of vibrationally excited levels of molecules (H: 0~14, D: 0~20)** is crucial because the difference of the ionization channel number via vibrationally excited levels is "one of the reasons for" the **different ionization rate coefficients.**[4]

## Reference

- [1] H. Nakano, *et al.*, Jpn. J. Appl. Phys, 59 SHHC09 (2020).
- [2] T. Shibata, *et al.*, J. Appl. Phys, 114 143301 (2013).
- [3] A. Hatayama, *et al.*, New J. Phys., 20 065001 (2018).
- [4] T. Shibata, *et al.*, 68 in this conference